CHALMERS
FINITE ELEMENT CENTER

PREPRINT 2003–09

A finite element method for the simulation of strong and weak discontinuities in elasticity

Anita Hansbo and Peter Hansbo

Chalmers Finite Element Center
CHALMERS UNIVERSITY OF TECHNOLOGY
Göteborg Sweden 2003

CHALMERS FINITE ELEMENT CENTER

Preprint 2003–09

A finite element method for the simulation of strong and weak discontinuities in elasticity

Anita Hansbo and Peter Hansbo

CHALMERS

Chalmers Finite Element Center
Chalmers University of Technology
SE–412 96 Göteborg Sweden
Göteborg, April 2003

A finite element method for the simulation of strong and weak discontinuities in elasticity
Anita Hansbo and Peter Hansbo
NO 2003–09
ISSN 1404–4382

Chalmers Finite Element Center
Chalmers University of Technology
SE–412 96 Göteborg
Sweden
Telephone: +46 (0)31 772 1000
Fax: +46 (0)31 772 3595
www.phi.chalmers.se

Printed in Sweden
Chalmers University of Technology
Göteborg, Sweden 2003

A FINITE ELEMENT METHOD FOR THE SIMULATION OF STRONG AND WEAK DISCONTINUITIES IN ELASTICITY

ANITA HANSBO AND PETER HANSBO

Abstract. In this paper we introduce and analyze a finite element method for elasticity problems with interfaces. The method allows for discontinuities, internal to the elements, in the approximation across the interface. The approach can handle both perfectly and imperfectly bonded interfaces in the same setting. For the case of linear elasticity, we show that optimal order of convergence holds without restrictions on the location of the interface relative to the mesh. We present numerical examples for the linear case as well as for contact and crack propagation model problems.

1. Introduction

As a model inclusion problem, we consider a linear elasticity problem in two or three dimensions with stiffness and/or Poisson's ratio discontinuous across a smooth internal interface. The interface is assumed to be perfectly bonded or, alternatively, imperfectly bonded with elastic spring-type interface conditions. We also consider a combination of the two to allow for self-contact, which yields a (non-linear) Signorini-type problem.

When solving such problems numerically using the standard finite element method, one usually takes the discontinuity of the data into account by enforcing mesh lines along the interface. If this is not done, suboptimal convergence behaviour will occur, cf. [1]. In contrast, the presented method is an extension of the unfitted finite element method presented in [3], allowing for discontinuities, internal to the elements, in the approximation across the interface separating the inclusion from the rest of the domain. This method is of optimal order; in particular we show second order convergence for the linear problems in L_2 for appropriately modified piecewise linears on a non-degenerate triangulation.

The possibility of incorporating discontinuities, either weak (discontinuous strains) or strong (discontinuous displacement fields) has been considered by several authors recently. Among the approaches most similar to ours we mention the partition of unity methods of Belytschko and co-workers [2] and of Wells and Sluys [10] (for an overview of recent work in this field, with many additional references, see Karihaloo and Xiao [4]).

Date: April 11, 2003.

Key words and phrases. Elastic inclusions, discontinuous Galerkin, Nitsche's method, a priori error estimates.

Anita Hansbo, Department of Informatics and Mathematics, University of Trollhättan Uddevalla, Box 957, S–461 39 Trollhättan, Sweden, *email*: anita.hansbo@htu.se

Peter Hansbo, Department of Solid Mechanics, Chalmers University of Technology, S–412 96 Göteborg, Sweden, *email*: hansbo@solid.chalmers.se.

In [10] only strong discontinuities are considered, since the jump is an explicit variable. The suboptimal convergence behaviour in the presence of weak discontinuities is thus still present with this method. By use of signed distance functions, the approach in [2] can handle weak discontinuities, with the strain jump as an explicit variable. In contrast, our approach is more like “traditional” finite element methods in that we only work with polynomial approximations, and neither the jump nor the strain jump is an explicit variable. The rate of convergence for the methods in [2, 10] is not known; to the best of our knowledge the present work is the first to show optimally convergent approximations of weak and strong discontinuities, using elements with internal discontinuities, (independent of the mesh) for elasticity problems.

The proposed finite element method and its convergence analysis for an incompressible linear elasticity problem with a perfectly or imperfectly bonded interface is presented in Section 2. In Section 3, we provide numerical examples that confirm the optimal convergence rate in the linear case and indicate the feasability of our approach applied to contact and fracture model problems, and finally, in Section 4, some concluding remarks are given.

2. A priori error analysis of the method for a linear model problem

In many cases, typically when the interface consists of a thin layer of adhesive, there is a need to model debonding at the interface. We begin by presenting an unfitted finite element method for this case. In order to have a linear model problem, we do not allow for self-contact; we shall return to this question in Section 3.2.

To define the problem, let Ω be a bounded domain in $\mathbb{R}^n$, $n = 2$ or $n = 3$, with convex polygonal boundary $\partial\Omega$ and an internal smooth boundary Γ dividing Ω into two open sets Ω_1 and Ω_2. For any sufficiently regular function $\boldsymbol{u} = [u_i]_{i=1}^n$ in $\Omega_1 \cup \Omega_2$ we define the jump of $\boldsymbol{u}$ on Γ by $[\boldsymbol{u}] := \boldsymbol{u}_1|_\Gamma - \boldsymbol{u}_2|_\Gamma$, where $\boldsymbol{u}_i = \boldsymbol{u}|_{\Omega_i}$ is the restriction of u to Ω_i. Conversely, for $\boldsymbol{u}_i$ defined in Ω_i we identify the pair $\{\boldsymbol{u}_1, \boldsymbol{u}_2\}$ with the function $\boldsymbol{u}$ which equals $\boldsymbol{u}_i$ on Ω_i. We consider the following elasticity problem with a discontinuity in the Lamé parameters across Γ: Find the displacement $\boldsymbol{u}$ and the symmetric stress tensor $\boldsymbol{\sigma} = [\sigma_{ij}]_{i,j=1}^n$ such that

$$\boldsymbol{\sigma} = \lambda\, \nabla \cdot \boldsymbol{u} \boldsymbol{I} + 2\mu \boldsymbol{\varepsilon}(\boldsymbol{u}) \quad \text{in} \quad \Omega_1 \cup \Omega_2, \tag{2.1}$$

$$-\nabla \cdot \boldsymbol{\sigma} = \boldsymbol{f} \quad \text{in} \quad \Omega_1 \cup \Omega_2, \tag{2.2}$$

$$\boldsymbol{u} = 0 \quad \text{on} \quad \partial\Omega, \tag{2.3}$$

$$[\boldsymbol{\sigma} \cdot \boldsymbol{n}] = 0 \quad \text{on} \quad \Gamma, \tag{2.4}$$

$$[\boldsymbol{u}] = -\boldsymbol{K} \boldsymbol{\sigma} \cdot \boldsymbol{n} \quad \text{on} \quad \Gamma. \tag{2.5}$$

Here λ and μ are the Lamé parameters, which we assume satisfy $0 < c < \mu < C$ and $0 < \lambda < C$ (thus we exclude the incompressible case). In terms of the modulus of elasticity, E, and Poisson's ratio, ν, we have

$$\lambda = \frac{\mathrm{E}\,\nu}{(1-2\nu)(1+\nu)}, \quad \mu = \frac{\mathrm{E}}{2\,(1+\nu)}.$$

Furthermore, $\boldsymbol{\varepsilon}(\boldsymbol{u}) = [\varepsilon_{ij}(\boldsymbol{u})]_{i,j=1}^n$ is the strain tensor with components

$$\varepsilon_{ij}(\boldsymbol{u}) = \frac{1}{2}\left(\frac{\partial u_i}{\partial x_j} + \frac{\partial u_j}{\partial x_i}\right),$$

$\nabla \cdot \boldsymbol{\sigma} = \left[\sum_{j=1}^2 \partial\sigma_{ij}/\partial x_j\right]_{i=1}^n$, $\boldsymbol{I} = [\delta_{ij}]_{i,j=1}^n$ with $\delta_{ij} = 1$ if $i = j$ and $\delta_{ij} = 0$ if $i \neq j$, $\boldsymbol{f}$ is a given load, and $\boldsymbol{n}$ is the outward pointing normal to Ω_1. Finally, $\boldsymbol{K}$ is a positive semi-definite tensor representing the compliancy of the interface. We consider here only isotropic elasticity on the interface, in which case we can write

$$\boldsymbol{K} = \alpha\,\boldsymbol{I} + (\beta - \alpha)\boldsymbol{n} \otimes \boldsymbol{n}, \quad \text{or} \quad K_{ij} = \alpha\delta_{ij} + (\beta - \alpha)n_i n_j,$$

with $\alpha \geq 0$ and $\beta \geq 0$ denoting the complicancy in the direction tangential and normal to the interface, respectively [11].

For a bounded open connected domain D we shall use standard Sobolev spaces $H^r(D)$ with norm $||\cdot||_{r,D}$ and spaces $H_0^r(D)$ with zero trace on ∂D. The inner products in $H^0(D) = L_2(D)$ is denoted $(\cdot,\cdot)_D$. For a bounded open set $G = \cup_{i=1}^2 D_i$, where D_i are open mutually disjoint components of G, we let $H^k(D_1 \cup D_2)$ denote the Sobolev space of functions in G such that $\boldsymbol{u}|_{D_i} \in [H^k(D_i)]^n$ with norm

$$\|\cdot\|_{k,D_1\cup D_2} = \left(\sum_{i=1}^2 \|\cdot\|_{k,D_i}^2\right)^{1/2}.$$

We assume that $\boldsymbol{f} \in [L_2(\Omega)]^n$ and, for simplicity, that λ and μ are constant in Ω_i, and that α and β are constant on Γ. Let the interface stiffness S be defined by

$$\boldsymbol{S} = \begin{cases} \boldsymbol{K}^{-1} & \text{for} \quad \alpha > 0, \beta > 0, \\ \alpha^{-2}\boldsymbol{K} = \alpha^{-1}(\boldsymbol{I} - \boldsymbol{n}\otimes\boldsymbol{n}) & \text{for} \quad \alpha > 0, \beta = 0, \\ \beta^{-2}\boldsymbol{K} = \beta^{-1}\boldsymbol{n}\otimes\boldsymbol{n} & \text{for} \quad \alpha = 0, \beta > 0, \\ 0 & \text{for} \quad \alpha = 0, \beta = 0, \end{cases}$$

and define the space V of test functions by

$$V = \{\boldsymbol{v} \in V_1 \times V_2 : [\boldsymbol{v}] = \boldsymbol{S}\boldsymbol{K}[\boldsymbol{v}]\} \quad \text{where} \quad V_i = \{\boldsymbol{v}_i \in [H^1(\Omega_i)]^n : \ \boldsymbol{v}_i|_{\partial\Omega} = 0\}.$$

Note that when $\boldsymbol{S} = \boldsymbol{K}^{-1}$ then $V = V_1 \times V_2$. A weak form of (2.1)–(2.5) may be formulated as follows: find $\boldsymbol{u} = (\boldsymbol{u}_1, \boldsymbol{u}_2) \in V$ such that

$$a_{\boldsymbol{S}}(\boldsymbol{u},\boldsymbol{v}) = L(\boldsymbol{v}) \quad \forall \boldsymbol{v} \in V. \tag{2.6}$$

Here,

$$a_{\boldsymbol{S}}(\boldsymbol{u},\boldsymbol{v}) := (\,\boldsymbol{\sigma}(\boldsymbol{u})\,,\boldsymbol{\varepsilon}(\boldsymbol{v})\,)_{\Omega_1\cup\Omega_2} + (\boldsymbol{S}\,[\boldsymbol{u}]\,,[\boldsymbol{v}]\,)_\Gamma,$$

where

$$(\,\boldsymbol{\sigma}\,,\boldsymbol{\varepsilon}\,)_{\Omega_i} = \int_{\Omega_i} \boldsymbol{\sigma} : \boldsymbol{\varepsilon}\,dx = \int_{\Omega_i} \sum_{ij} \sigma_{ij}\varepsilon_{ij}\,dx,$$

and

$$L(\boldsymbol{v}) := (\boldsymbol{f},\boldsymbol{v})_\Omega.$$

This problem has a unique solution which is in H^2 on each subdomain, cf. Leguillon and Sanchez-Palencia [5].

2.1. **The finite element method.** In a standard conforming finite element method, the possibility of jumps in strain across the interface can be taken into account by letting Γ coincide with mesh lines. We will instead follow [3] and solve (2.1)–(2.5) approximately using piecewise linear finite elements on a family of conforming triangulations T_h of Ω which are independent of the location of the interface Γ. Instead, we shall allow the approximation to be *discontinuous inside elements which intersect the interface.* For the problem under consideration, this approach has the additional advantage of allowing the same approximation for the solution of both the perfectly bonded and the imperfectly bonded interface problem.

We will now explain how elements with internal discontinuities are constructed from standard (in the simplest case linear) finite elements on a triangular grid. Consider first an element K which is intersected by the interface and thus consists of one part $K_1 := \Omega_1 \cap K$ in Ω_1, and another part $K_2 := \Omega_2 \cap K$ in Ω_2. FE functions ϕ with internal discontinuities will be linear on each part but discontinuous over the interface. Thus

$$\phi = \begin{cases} \phi_1 & \text{in } K_1 \\ \phi_2 & \text{in } K_2 \end{cases}$$

Since ϕ is discontinuous over the interface, there exist no relation between (the degrees of freedoms for) ϕ_1 and ϕ_2. To determine the linear function ϕ_1 on K_1, one needs three degrees of freedom. Notice that we may very well choose represent ϕ_1 by the nodal values at the corners of K (strictly speaking: represent ϕ_1 by the nodal values of its unique linear extension to K), even though we think of ϕ_1 as not being defined on K_2. Likewise, ϕ_2 lives only on K_2 but we may still represent it by its values in the same corner node. Thus the piecewise linear element with an internal discontinuity has six degrees of freedom.

A FE basis with internal discontinuities over the interface may be constructed from a standard FE basis as follows. Consider a standard linear basis function ψ^j, $j = 1, 2$ or 3, that takes on the value one in one of the nodes x_j of K and zero in the other. This basis function corresponds to two basis functions with internal discontinuities:

$$\psi_1^j = \begin{cases} \psi^j & \text{in } K_1, \\ 0 & \text{in } K_2, \end{cases} \quad , \quad \text{and} \quad \psi_2^j = \begin{cases} 0 & \text{in } K_1, \\ \psi^j & \text{in } K_2. \end{cases}$$

In all we have six new basis functions on the linear element with an internal discontinuity, one for each degree of freedom.

By similar reasoning, we see that from any standard finite element in 2D or 3D, a corresponding element with internal discontinuity across an interface may be constructed. Furthermore, one may do this using the nodes on the standard element to represent the degrees of freedom. The number of degrees of freedom for the element with an internal discontinuitiy is twice that of the original element, and a FEM basis may be constructed by considering two copies of the original bases functions, restricted to Ω_1 and Ω_2, respectively. The points of intersection between the element edges and the interface are *not* used to represent the new basis function, and the geometry of the interface and the element parts does *not* come into play until when integrating the terms in the bilinear form.

Formalizing this tutorial explanation, we shall seek a discrete solution $\boldsymbol{U} = (\boldsymbol{U}_1, \boldsymbol{U}_2)$ in the space $V^h = V_1^h \times V_2^h$, where

$$V_i^h = \{\boldsymbol{\phi}_i \in [H^1(\Omega_i)]^n : \ \boldsymbol{\phi}_i|_{K_i} \text{ is linear}, \quad \boldsymbol{\phi}_i|_{\partial\Omega} = 0\}.$$

The functions in V^h may be discontinuous across Γ, and the interface conditions will be imposed weakly.

Now, for $\alpha > 0, \beta > 0$, the continuous problem (2.6) could simply be approximated by a straightforward use of the discrete space V^h: Find $\boldsymbol{U} \in V^h$ such that

$$a_{\boldsymbol{S}}(\boldsymbol{U}, \boldsymbol{\phi}) := (\, \boldsymbol{\sigma}(\boldsymbol{u}) \,, \boldsymbol{\varepsilon}(\boldsymbol{v}) \,)_{\Omega_1 \cup \Omega_2} + (\boldsymbol{S}\,[\boldsymbol{u}] \,, [\boldsymbol{v}] \,)_\Gamma = L(\boldsymbol{\phi}) \quad \forall \boldsymbol{\phi} \in V^h. \tag{2.7}$$

However, in the case of small parameters α and β this would lead to a badly conditioned problem, and, furthermore, the question of locking would have to be considered. The formulation would also fail in the limit case $\alpha = 0$ or $\beta = 0$ since the functions in V^h do not fulfill any interface conditions over Γ. On the other hand, for the case $\alpha = 0$ and $\beta = 0$, the bounday conditions may still be imposed weakly over the interface by using a Nitsche [6] type method like in [3].

We shall here investigate a more general approach that builds on ideas proposed in another context by by Stenberg [7]. To this end, we shall need to define a numerical stress at the interface, and this will first be done by considering any convex combination of the stresses at each side of the interface. More precisely, given $\kappa = (\kappa_1, \kappa_2)$ with $0 \le \kappa_1 \le 1$, $\kappa_2 = 1 - \kappa_1$, and $\boldsymbol{\phi} = (\boldsymbol{\phi}_1, \boldsymbol{\phi}_2)$ on Ω, we let

$$\{\boldsymbol{\sigma}(\boldsymbol{\phi}) \cdot \boldsymbol{n}\} := (\kappa_1 \boldsymbol{\sigma}_1(\boldsymbol{\phi}_1) \cdot \boldsymbol{n} + \kappa_2 \boldsymbol{\sigma}_2(\boldsymbol{\phi}_2) \cdot \boldsymbol{n}) \quad \text{at } \Gamma.$$

The proposed method reads: Find $\boldsymbol{U} \in V^h$ such that

$$a_{\boldsymbol{S}_h}(\boldsymbol{U}, \boldsymbol{\phi}) = L(\boldsymbol{\phi}), \quad \forall \boldsymbol{\phi} \in V^h, \tag{2.8}$$

where

$$\begin{aligned} a_{\boldsymbol{S}_h}(\boldsymbol{U}, \boldsymbol{\phi}) \ :=\ & (\, \boldsymbol{\sigma}(\boldsymbol{U}) \,, \boldsymbol{\varepsilon}(\boldsymbol{\phi}) \,)_{\Omega_1 \cup \Omega_2} \\ & -(\, [\boldsymbol{U}] + \boldsymbol{K}\,\{\boldsymbol{\sigma}(\boldsymbol{U}) \cdot \boldsymbol{n}\} \,, \{\boldsymbol{\sigma}(\boldsymbol{\phi}) \cdot \boldsymbol{n}\} \,)_\Gamma \\ & -(\, \{\boldsymbol{\sigma}(\boldsymbol{U}) \cdot \boldsymbol{n}\} \,, [\boldsymbol{\phi}] + \boldsymbol{K}\,\{\boldsymbol{\sigma}(\boldsymbol{\phi}) \cdot \boldsymbol{n}\} \,)_\Gamma \\ & +(\, \boldsymbol{K}\{\boldsymbol{\sigma}(\boldsymbol{U}) \cdot \boldsymbol{n}\} \,, \{\boldsymbol{\sigma}(\boldsymbol{\phi}) \cdot \boldsymbol{n}\} \,)_\Gamma \\ & +(\, \boldsymbol{S}_h([\boldsymbol{U}] + \boldsymbol{K}\{\boldsymbol{\sigma}(\boldsymbol{U}) \cdot \boldsymbol{n}\}) \,, [\boldsymbol{\phi}] + \boldsymbol{K}\{\boldsymbol{\sigma}(\boldsymbol{\phi}) \cdot \boldsymbol{n}\} \,)_\Gamma \end{aligned}$$

with $\boldsymbol{S}_h = (h/\delta + \boldsymbol{K})^{-1}$ chosen with an appropriate mesh and problem dependent penalty parameter δ (see Lemma 4 below), and with appropriate mesh and geometry dependent weights κ to be defined below (see (2.10)).

We remark that the form $a_{\boldsymbol{S}_h}(\cdot, \cdot)$ coincides with $a_{\boldsymbol{S}}(\cdot, \cdot)$ in the limit case $\boldsymbol{S}_h = \boldsymbol{K}^{-1}$. Note also that, in the case $\boldsymbol{K} = 0$, $a_{\boldsymbol{S}_h}(\cdot, \cdot)$ coincides with the standard Nitsche form used in [3]. Thus the proposed method contains and extends these methods into one single method for all $\alpha \ge 0, \beta \ge 0$.

The following consistency relation follows directly by use of Green's formula.

Lemma 1. *The discrete problem* (2.8) *is consistent in the sense that, for* $\boldsymbol{u}$ *solving* (2.1)–(2.5)*,*

$$a_{\boldsymbol{S}_h}(\boldsymbol{u}, \boldsymbol{\phi}) = L(\boldsymbol{\phi}), \quad \forall \boldsymbol{\phi} \in V^h.$$

An immediate consequence of Lemma 1 is the orthogonality condition

$$a_{\boldsymbol{S}_h}(\boldsymbol{u} - \boldsymbol{U}, \boldsymbol{\phi}) = 0, \quad \forall \boldsymbol{\phi} \in V^h. \tag{2.9}$$

To get a stable method for elements with internal discontinuities, further conditions on the combinations of numerical stresses must be imposed.

2.2. **Mesh assumptions and definition of the numerical stress at the interface.** We will use the following notation for mesh related quantities. Let h_K be the diameter of K and $h_{\max} = \max_{K \in T_h} h_K$. For any element K, let $K_i = K \cap \Omega_i$ denote the part of K in Ω_i. By $G_h := \{K \in T_h : K \cap \Gamma \neq \emptyset\}$ we denote the set of elements that are intersected by the interface. For an element $K \in G_h$, let $\Gamma_K := \Gamma \cap K$ be the part of Γ in K. By $h := h(\boldsymbol{x})$ we denote the piecewise discontinuous function that fulfills $h|_K = h_K$.

As in [3], we make the following assumptions regarding the mesh and the interface, here formulated for the case of three space dimensions.

A1: The triangulation is non-degenerate, i.e.,

$$h_K / \rho_K \leq C \quad \forall K \in T_h$$

where h_K is the diameter of K and ρ_K is the diameter of the largest ball contained in K.

A2: The intersection of Γ and the boundary of $K \in G_h$ is a connected curve. (This implies that Γ divides each $K \in G_h$ into two parts and intersects three or four edges of K in one point each.)

A3: Take a plane through three of the points of intersection between Γ and the edges of K, and let $\Gamma_{K,h}$ be the intersection between K and this plane. Then Γ_K is a function on $\Gamma_{K,h}$ for some choise of points of intersection; thus

$$\Gamma_K = \{(\xi, \eta, \zeta) : (\xi, \eta, 0) \in \Gamma_{K,h}, \zeta = \delta(\xi, \eta)\}$$

in local coordinates (ξ, η, ζ).

Since the curvature of Γ is bounded, the assumptions A2 and A3 are always fulfilled on some sufficiently fine mesh. Thus the assumptions are natural in that they ensure that the curvature of the interface is well resolved by the mesh. The method may be formulated and analysed under less restrictive conditions, e.g. conditions that allow for the interface to coincide with a twodimensional subset of a side of an element. Naturally, such less restrictive conditions on the mesh yields a method which requires a more elaborate implementation as more cases to consider are introduced.

Since the interface Γ may intersect three or four edges of a tetrahedron arbitrarily, the size of the parts K_i are not fully characterized by the meshsize parameters. We therefore introduce the function $\kappa = (\kappa_1, \kappa_2)$ defined on the interior of each element by

$$\kappa_1|_K = \left\{ \begin{array}{ll} 1 & \text{if} \quad |K_1| \geq |K_2|, \\ 0 & \text{if} \quad |K_1| < |K_2| \end{array} \right. , \qquad \text{and} \qquad \kappa_2(x) = |1 - \kappa_1(x)|, \tag{2.10}$$

where $|K| := \text{meas}\, K$.

2.3. **Approximation properties of V^h.** Recall that G_h denotes the set of elements that are intersected by the interface. We will use the following mesh dependent norms:

$$\|\boldsymbol{v}\|^2_{1/2,h,\Gamma} := \sum_{K\in G_h} h_K^{-1}\|\boldsymbol{v}\|^2_{0,\Gamma_K},$$

$$\|\boldsymbol{v}\|^2_{-1/2,h,\Gamma} := \sum_{K\in G_h} h_K\|\boldsymbol{v}\|^2_{0,\Gamma_K},$$

and, with $\lambda_{\text{m}} := \max_\Omega \lambda$ and $\mu_{\text{m}} := \max_\Omega \mu$,

$$\begin{aligned} |||\boldsymbol{v}|||_h^2 \;\; := \;\; & (\,\boldsymbol{\sigma}(\boldsymbol{v}_i)\,,\boldsymbol{\varepsilon}(\boldsymbol{v}_i)\,)_{\Omega_1\cup\Omega_2} + (2\mu_{\text{m}}+3\lambda_{\text{m}})\|[\boldsymbol{v}] + \boldsymbol{K}\{\boldsymbol{\sigma}(\boldsymbol{v})\}\cdot\boldsymbol{n}\|^2_{1/2,h,\Gamma} \\ & + \frac{1}{2\mu_{\text{m}}+3\lambda_{\text{m}}}\|\{\boldsymbol{\sigma}(\boldsymbol{v})\}\cdot\boldsymbol{n}\|^2_{-1/2,h,\Gamma}. \end{aligned}$$

We note for future reference that

$$(\boldsymbol{u},\boldsymbol{v})_\Gamma \le \|\boldsymbol{u}\|_{1/2,h,\Gamma}\|\boldsymbol{v}\|_{-1/2,h,\Gamma}. \tag{2.11}$$

To show that functions in V^h approximates functions $v \in H^1_0(\Omega)\cap H^2(\Omega_1\cup\Omega_2)$ to the order h in the norm $|||\cdot|||_h$, we construct an interpolant of $\boldsymbol{v}$ by nodal interpolants of H^2-extensions of $\boldsymbol{v}_1$ and $\boldsymbol{v}_2$ as follows. Choose extensions operators $\mathsf{E}_i : [H^2(\Omega_i)]^n \to [H^2(\Omega)]^n$ such that $(\mathsf{E}_i\boldsymbol{w})|_{\Omega_i} = \boldsymbol{w}$ and

$$\|\mathsf{E}_i\boldsymbol{w}\|_{s,\Omega} \le C\|\boldsymbol{w}\|_{s,\Omega_i} \quad \forall \boldsymbol{w}\in[H^s(\Omega_i)]^n, \quad s=0,1,2. \tag{2.12}$$

Let I_h be the standard Lagrangian nodal interpolation operator and define

$$I_h^*\boldsymbol{v} := (I_{h,1}^*\boldsymbol{v}_1, I_{h,2}^*\boldsymbol{v}_2) \quad \text{where } I_{h,i}^*\boldsymbol{v}_i := (I_h\mathsf{E}_i\boldsymbol{v}_i)|_{\Omega_i}. \tag{2.13}$$

The following theorem is valid.

Theorem 1. *Let I_h^* be an interpolation operator defined as in* (2.13)*. Then*

$$|||\boldsymbol{v} - I_h^*\boldsymbol{v}||| \le C_A h_{\max}\|\boldsymbol{v}\|_{2,\Omega_1\cup\Omega_2}, \quad \forall \boldsymbol{v}\in[H^1_0(\Omega)]^n\cap[H^2(\Omega_1\cup\Omega_2)]^n.$$

The proof of this theorem may be found in [3] and hinges on the trace inequality in Lemma 2 below. This is a variant of the well known trace inequality

$$\|w\|^2_{0,\partial\tilde K} \le C\|w\|_{0,\tilde K}\|w\|_{1,\tilde K}, \quad \forall w\in H^1(\tilde K). \tag{2.14}$$

on a reference element $\tilde K$. The crucial fact is that the constant in (2.15) is independent of the location of the interface relative to the mesh. We give here a proof of this Lemma which is simpler than the proof in [3].

Lemma 2. *Map a tetrahedron $K\in G_h$ onto the unit reference tetrahedron $\tilde K$ by an affine map and denote by $\tilde\Gamma_{\tilde K}$ the corresponding image of Γ_K. Under assumptions A1–A3 of Section 2.1 there exist a constant C, depending on Γ but independent of the mesh, such that*

$$\|w\|^2_{0,\tilde\Gamma_{\tilde K}} \le C\|w\|_{0,\tilde K}\|w\|_{1,\tilde K}, \quad \forall w\in H^1(\tilde K). \tag{2.15}$$

PROOF. Recall that

$$\Gamma_K = \{(\xi,\eta,\zeta) : (\xi,\eta,0) \in \Gamma_{K,h}, \zeta = \delta(\xi,\eta)\}.$$

On the reference element we may write, using again (ξ,η,ζ) to denote local coordinates on $\tilde{K}$,

$$\tilde{\Gamma}_{\tilde{K}} = \{(\xi,\eta,\zeta) : (\xi,\eta,0) \in \tilde{\Gamma}_{\tilde{K},h}, \zeta = \tilde{\delta}(\xi,\eta)\}.$$

We let $\mathbf{n}$ denote the outward pointing unit normal of $\tilde{K}_1$ and note that for its component in the ζ-direction we have $n_\zeta = \pm(1+|\nabla\tilde{\delta}|^2)^{-1/2}$ on $\tilde{\Gamma}$. By the divergence theorem,

$$\begin{aligned} 2\int_{\tilde{K}_i} w\frac{\partial w}{\partial \zeta}\, dV &= \int_{\tilde{K}_i} \text{div }(0,0,w^2)\, dV = \int_{\partial\tilde{K}_i} \mathbf{n}\cdot(0,0,w^2)\, dA \\ &= \int_{\tilde{\Gamma}_{\tilde{K}}} w^2(1+|\nabla\tilde{\delta}|^2)^{-1/2}\, dA + \int_{\partial\tilde{K}_1\setminus\tilde{\Gamma}_{\tilde{K}}} n_\zeta w^2\, dA. \end{aligned} \tag{2.16}$$

Since the interface is smooth and bounded and the mesh is non-degenerate, $|\delta'_\xi|^2 + |\delta'_\eta|^2 \le Ch_K^2$, and thus $|\nabla\tilde{\delta}| \le C$, which implies that

$$\|w\|^2_{0,\tilde{\Gamma}_{\tilde{K}}} \le C\int_{\tilde{\Gamma}_{\tilde{K}}} w^2(1+|\nabla\tilde{\delta}|^2)^{-1/2}\, dA.$$

By (2.16) we thus find, using Cauchy-Schwarz' inequality, that

$$\|w\|^2_{0,\tilde{\Gamma}_{\tilde{K}}} \le 2\|w\|_{0,\tilde{K}_1}\|w\|_{1,\tilde{K}_1} + \|w\|^2_{0,\partial\tilde{K}_1\setminus\tilde{\Gamma}_{\tilde{K}}}.$$

The result of the lemma now follows from (2.14). □

2.4. *A priori* error estimates.

In order to show that the bilinear form $a_{\boldsymbol{S}_h}(\cdot,\cdot)$ is coercive on V^h, we will need the following inverse inequality.

Lemma 3. *For $\boldsymbol{\phi} \in V^h$, the following inverse inequality holds:*

$$\|\{\boldsymbol{\sigma}(\boldsymbol{\phi})\}\|^2_{-1/2,h,\Gamma} \le C_I\|\boldsymbol{\sigma}(\boldsymbol{\phi})\|^2_{0,\Omega_1\cup\Omega_2}.$$

PROOF. Since $\boldsymbol{\phi} \in V^h$ is linear on K_i, $\boldsymbol{\sigma}(\boldsymbol{\phi}_i)$ is constant and we have

$$\begin{aligned} h_K\|\kappa_i\boldsymbol{\sigma}(\boldsymbol{\phi}_i)\|^2_{0,\Gamma_K} &\le h_K\kappa_i^2|\Gamma_K|\,|\boldsymbol{\sigma}(\boldsymbol{\phi}_i)|^2 = h_K\kappa_i^2\frac{|\Gamma_K|}{|K_i|}\,\|\boldsymbol{\sigma}(\boldsymbol{\phi}_i)\|^2_{0,K_i} \\ &= h_K\frac{|\Gamma_K|\,|K_i|}{|K|^2}\,\|\boldsymbol{\sigma}(\boldsymbol{\phi}_i)\|^2_{0,K_i} \le C\|\boldsymbol{\sigma}(\boldsymbol{\phi}_i)\|^2_{0,K_i}. \end{aligned}$$

In the last step above we have used that $|\Gamma_K| \le h_K$, $|K_i| \le h_K^2$, and, since the mesh is nondegenerate, $|K| \ge ch_K^2$. The result follows by summation over the elements. □

Lemma 4. *The discrete form $a_{\boldsymbol{S}_h}(\cdot,\cdot)$ is coercive on V^h w.r.t. $|||\cdot|||_h$, i.e.,*

$$a_{\boldsymbol{S}_h}(\boldsymbol{v},\boldsymbol{v}) \ge C|||\boldsymbol{v}|||_h^2 \quad \forall \boldsymbol{v} \in V^h,$$

for $\boldsymbol{S}_h = (h/\delta + \boldsymbol{K})^{-1}$ with $\delta \ge 8\,C_I(2\mu_{\text{m}} + 3\lambda_{\text{m}})$. It is also continuous, i.e.,

$$a_{\boldsymbol{S}_h}(\boldsymbol{u},\boldsymbol{v}) \le C|||\boldsymbol{u}|||_h|||\boldsymbol{v}|||_h \quad \forall \boldsymbol{u},\boldsymbol{v} \in V.$$

PROOF. Continuity follows directly from the definitions. To show coercivity, we first note that the stress-strain relation can be inverted to yield

$$\boldsymbol{\varepsilon} = \frac{1}{2\mu}\left(\boldsymbol{\sigma} - \frac{\lambda}{3\lambda+2\mu}\mathrm{tr}\,\boldsymbol{\sigma}\,\boldsymbol{I}\right) = \frac{1}{2\mu}\boldsymbol{\sigma}^D + \frac{1}{9\lambda+6\mu}\mathrm{tr}\,\boldsymbol{\sigma}\,\boldsymbol{I},$$

where $\boldsymbol{\sigma}^D := \boldsymbol{\sigma} - \mathrm{tr}\,\boldsymbol{\sigma}\,\boldsymbol{I}/3$ and $\mathrm{tr}\,\boldsymbol{\sigma} := \sum_i \sigma_{ii}$, and thus we have that

$$\boldsymbol{\sigma} : \boldsymbol{\varepsilon} = \frac{1}{2\mu}\boldsymbol{\sigma}^D : \boldsymbol{\sigma}^D + \frac{1}{9\lambda+6\mu}(\mathrm{tr}\,\boldsymbol{\sigma})^2$$

and

$$\boldsymbol{\sigma} : \boldsymbol{\sigma} = \boldsymbol{\sigma}^D : \boldsymbol{\sigma}^D + \frac{1}{3}(\mathrm{tr}\,\boldsymbol{\sigma})^2,$$

so that

$$\boldsymbol{\sigma} : \boldsymbol{\sigma} \leq (2\mu + 3\lambda)\,\boldsymbol{\sigma} : \boldsymbol{\varepsilon}. \tag{2.17}$$

By definition of $a_{\boldsymbol{S}_h}(\cdot,\cdot)$, we have

$$\begin{aligned} a_{\boldsymbol{S}_h}(\boldsymbol{v},\boldsymbol{v}) \;=\;& (\boldsymbol{\sigma}(\boldsymbol{v}),\boldsymbol{\varepsilon}(\boldsymbol{v}))_{\Omega_1\cup\Omega_2} - 2([\boldsymbol{v}] + \boldsymbol{K}\{\boldsymbol{n}\cdot\boldsymbol{\sigma}(\boldsymbol{v})\},\{\boldsymbol{n}\cdot\boldsymbol{\sigma}(\boldsymbol{v})\})_\Gamma \\ & +(\{\boldsymbol{n}\cdot\boldsymbol{\sigma}(\boldsymbol{v})\},\boldsymbol{K}\{\boldsymbol{n}\cdot\boldsymbol{\sigma}(\boldsymbol{v})\})_\Gamma \\ & +(\boldsymbol{S}_h([\boldsymbol{v}] + \boldsymbol{K}\{\boldsymbol{n}\cdot\boldsymbol{\sigma}(\boldsymbol{v})\}),[\boldsymbol{v}] + \boldsymbol{K}\{\boldsymbol{n}\cdot\boldsymbol{\sigma}(\boldsymbol{v})\})_\Gamma. \end{aligned} \tag{2.18}$$

We consider first the second term on the right-hand side. For any symmetric positive definite matrix $\boldsymbol{M}$ it follows from Cauchy-Schwarz inequality that

$$\begin{aligned} & 2([\boldsymbol{v}] + \boldsymbol{K}\{\boldsymbol{n}\cdot\boldsymbol{\sigma}(\boldsymbol{v})\},\{\boldsymbol{n}\cdot\boldsymbol{\sigma}(\boldsymbol{v})\})_\Gamma \\ &\quad = 2(\sqrt{\boldsymbol{M}h^{-1}}([\boldsymbol{v}] + \boldsymbol{K}\{\boldsymbol{n}\cdot\boldsymbol{\sigma}(\boldsymbol{v})\}),\sqrt{\boldsymbol{M}^{-1}h}\{\boldsymbol{n}\cdot\boldsymbol{\sigma}(\boldsymbol{v})\})_\Gamma \\ &\quad \leq \|\sqrt{\boldsymbol{M}^{-1}h}\{\boldsymbol{\sigma}(\boldsymbol{v})\cdot\boldsymbol{n}\}\|_{0,\Gamma}^2 + \|\sqrt{\boldsymbol{M}h^{-1}}([\boldsymbol{v}] + \boldsymbol{K}\{\boldsymbol{n}\cdot\boldsymbol{\sigma}(\boldsymbol{v})\})\|_{0,\Gamma}^2. \end{aligned}$$

We now set $\boldsymbol{M} = h(h/\delta_0 + \boldsymbol{K})^{-1}$ with $\delta_0 > 0$ so that

$$\begin{aligned} \|\sqrt{\boldsymbol{M}^{-1}h}\{\boldsymbol{\sigma}(\boldsymbol{v})\cdot\boldsymbol{n}\}\|_{0,\Gamma}^2 \;=\;& (\delta_0^{-1}h\{\boldsymbol{\sigma}(\boldsymbol{v})\cdot\boldsymbol{n}\},\{\boldsymbol{\sigma}(\boldsymbol{v})\cdot\boldsymbol{n}\})_{0,\Gamma} \\ & +(\boldsymbol{K}\{\boldsymbol{\sigma}(\boldsymbol{v})\cdot\boldsymbol{n}\},\{\boldsymbol{\sigma}(\boldsymbol{v})\cdot\boldsymbol{n}\})_{0,\Gamma}. \end{aligned}$$

By Lemma 3 and (2.17) we find that

$$\begin{aligned} (\delta_0^{-1}h\{\boldsymbol{\sigma}(\boldsymbol{v})\cdot\boldsymbol{n}\},\{\boldsymbol{\sigma}(\boldsymbol{v})\cdot\boldsymbol{n}\})_{0,\Gamma} \;\leq\;& \delta_0^{-1}C_I\|\boldsymbol{\sigma}(\boldsymbol{v})\|_{0,\Omega_1\cup\Omega_2}^2 \\ \leq\;& \delta_0^{-1}C_I(2\mu_{\mathrm{m}} + 3\lambda_{\mathrm{m}})(\boldsymbol{\sigma}(\boldsymbol{v}),\boldsymbol{\varepsilon}(\boldsymbol{v}))_{0,\Omega_1\cup\Omega_2}. \end{aligned}$$

Applying these estimates to the second term in (2.18) and collecting the terms we find that

$$\begin{aligned} & a_{\boldsymbol{S}_h}(\boldsymbol{v},\boldsymbol{v}) \geq (1 - 2\delta_0^{-1}C_I(2\mu_{\mathrm{m}} + 3\lambda_{\mathrm{m}}))(\boldsymbol{\sigma}(\boldsymbol{v}),\boldsymbol{\varepsilon}(\boldsymbol{v}))_{\Omega_1\cup\Omega_2} \\ &\quad +(\delta_0^{-1}h\{\boldsymbol{\sigma}(\boldsymbol{v})\cdot\boldsymbol{n}\},\{\boldsymbol{\sigma}(\boldsymbol{v})\cdot\boldsymbol{n}\})_{0,\Gamma} \\ &\quad +((\boldsymbol{S}_h - (h/\delta_0 + \boldsymbol{K})^{-1})([\boldsymbol{v}] + \boldsymbol{K}\{\boldsymbol{n}\cdot\boldsymbol{\sigma}(\boldsymbol{v})\}),[\boldsymbol{v}] + \boldsymbol{K}\{\boldsymbol{n}\cdot\boldsymbol{\sigma}(\boldsymbol{v})\})_\Gamma. \end{aligned}$$

We now choose $\delta_0 = 4\,C_I(2\mu_{\mathrm{m}} + 3\lambda_{\mathrm{m}})$ so that the first two terms on the right-hand side are bounded from below as desired. It remains to show that the matrix

$$\boldsymbol{A} := (h/\delta + \boldsymbol{K})^{-1} - (h/\delta_0 + \boldsymbol{K})^{-1}$$

is positive definite with eigenvalues uniformly bounded from below for all δ with $2\delta_0 \leq \delta \leq C$. To this end, note first that $\boldsymbol{A}$ is a rational function of $\boldsymbol{K}$, $\boldsymbol{A} = r(\boldsymbol{K})$. Now, from elementary spectral theory, $\boldsymbol{A}$ and $\boldsymbol{K}$ have identical eigenvectors and any eigenvalue a of $\boldsymbol{A}$ is related to the eigenvalues k of $\boldsymbol{K}$ by $a = r(k)$. Thus,

$$a = r(k) = \frac{1}{1/\delta + k} - \frac{1}{1/\delta_0 + k} = \frac{\delta_0^{-1} - \delta^{-1}}{(1/\delta + k)(1/\delta_0 + k)}.$$

By our assumptions, δ_0 is bounded from above and below. Now, if $\delta = 2\delta_0$ then, since k is bounded from above,

$$(1/\delta + k)(1/\delta_0 + k) \leq (1/\delta_0 + k)^2 \leq C$$

and

$$\delta_0^{-1} - \delta^{-1} \geq 1/\delta \geq c \geq 0.$$

Thus the eigenvalues of $\boldsymbol{A}$ are bounded from below and the result follows. □

Theorem 2. *Under assumptions A1–A3 of Section 2.1, and for* $\boldsymbol{U}$ *solving* (2.8) *and* $\boldsymbol{u}$ *solving* (2.1)–(2.5)*, the following* a priori *error estimates hold:*

$$|||\boldsymbol{u} - \boldsymbol{U}|||_h \leq C h_{\max} \|\boldsymbol{u}\|_{2,\Omega_1\cup\Omega_2} \tag{2.19}$$

and

$$\|\boldsymbol{u} - \boldsymbol{U}\|_{0,\Omega} \leq C h_{\max}^2 \|\boldsymbol{u}\|_{2,\Omega_1\cup\Omega_2} \tag{2.20}$$

PROOF. By Lemma 4 and orthogonality, we have that

$$\begin{aligned} |||\boldsymbol{U} - \boldsymbol{v}|||_h^2 \leq C a_{\boldsymbol{S}_h}(\boldsymbol{U} - \boldsymbol{v}, \boldsymbol{U} - \boldsymbol{v}) &= C a_{\boldsymbol{S}_h}(\boldsymbol{u} - \boldsymbol{v}, \boldsymbol{U} - \boldsymbol{v}) \\ &\leq C |||\boldsymbol{u} - \boldsymbol{v}|||_h \; |||\boldsymbol{U} - \boldsymbol{v}|||_h, \end{aligned}$$

and it follows that

$$|||\boldsymbol{u} - \boldsymbol{U}|||_h \leq C |||\boldsymbol{u} - \boldsymbol{v}|||_h \quad \forall \boldsymbol{v} \in V^h.$$

Taking $\boldsymbol{v} = I_h^* \boldsymbol{u}$ and invoking the interpolation result of Theorem 1, (2.19) follows.

For (2.20) we use a duality argument. Define $\boldsymbol{z} = (\boldsymbol{z}_1, \boldsymbol{z}_2)$ by

$$\begin{aligned} -\nabla \cdot \boldsymbol{\sigma}(\boldsymbol{z}) &= \boldsymbol{e} \quad \text{in} \quad \Omega_1 \cup \Omega_2, \\ \boldsymbol{z}_i &= 0 \quad \text{on} \quad \partial\Omega \cap \partial\Omega_i, \\ [\boldsymbol{\sigma}(\boldsymbol{z}) \cdot \boldsymbol{n}] &= 0 \quad \text{on} \quad \Gamma, \\ [\boldsymbol{z}] + \boldsymbol{K}\boldsymbol{\sigma}(\boldsymbol{z}) \cdot \boldsymbol{n} &= 0 \quad \text{on} \quad \Gamma. \end{aligned} \tag{2.21}$$

where $\boldsymbol{\sigma}(\boldsymbol{z}) := 2\mu\boldsymbol{\varepsilon}(\boldsymbol{z}) + \lambda \; \nabla \cdot \boldsymbol{z} \boldsymbol{I}$ and $\boldsymbol{e} := \boldsymbol{u} - \boldsymbol{U}$. By Green's formula we have that

$$\begin{aligned} \|\boldsymbol{e}\|_{0,\Omega}^2 &= -\left(\nabla \cdot \boldsymbol{\sigma}(\boldsymbol{z}), \boldsymbol{e}\right)_{\Omega_1\cup\Omega_2} \\ &= \left(\boldsymbol{\sigma}(\boldsymbol{z}), \boldsymbol{\varepsilon}(\boldsymbol{e})\right)_\Omega - (\boldsymbol{\sigma}(\boldsymbol{z}_1) \cdot \boldsymbol{n}, \boldsymbol{e}_1) + (\boldsymbol{\sigma}(\boldsymbol{z}_2) \cdot \boldsymbol{n}, \boldsymbol{e}_2) \\ &= \left(\boldsymbol{\sigma}(\boldsymbol{z}), \boldsymbol{\varepsilon}(\boldsymbol{e})\right)_\Omega - \left(\{\boldsymbol{\sigma}(\boldsymbol{z}) \cdot \boldsymbol{n}\}, [\boldsymbol{e}]\right)_\Gamma \\ &= a_{\boldsymbol{S}_h}(\boldsymbol{z}, \boldsymbol{e}), \end{aligned}$$

since $[\boldsymbol{z}] + \boldsymbol{K}\{\boldsymbol{\sigma}(\boldsymbol{z}) \cdot \boldsymbol{n}\} = 0$. Thus, using the symmetry of $a_{\boldsymbol{S}_h}(\cdot,\cdot)$ and applying the orthogonality relation (2.9) and Theorem 1, we find that

$$
\begin{aligned}
\|\boldsymbol{e}\|^2_{0,\Omega} &= a_{\boldsymbol{S}_h}(\boldsymbol{z} - I_h\boldsymbol{z}, \boldsymbol{e}) \le C|||\boldsymbol{z} - I_h\boldsymbol{z}|||_h \, |||\boldsymbol{e}|||_h \\
&\le Ch_{\max}\|\boldsymbol{z}\|_{2,\Omega_1\cup\Omega_2}|||\boldsymbol{e}|||_h.
\end{aligned} \tag{2.22}
$$

Finally, by elliptic regularity, cf. [5], we have $\|\boldsymbol{z}\|_{2,\Omega_1\cup\Omega_2} \le C\|\boldsymbol{e}\|_{0,\Omega}$, whence the estimate (2.20) follows from (2.22) and (2.19). □

3. Numerical examples

In this Section, we will give some numerical examples of the capabilities and behaviour of our approach. Besides the inclusion problem discussed above, we shall also consider an elastic contact problem and a simple crack propagation model with hardening at the interface. We emphasize that the error estimates from the preceding section cannot be expected to hold for these applications due to lack of regularity of the solution.

The basic implementation issues in this method were discussed above and further in [3]. Below we shall give some additional details concerning the implementation of the contact and crack propagation problems.

3.1. **Convergence.** In order to show the convergence of our method in a smooth case, we considered an inclusion problem with exact solution from Sukumar et al. [8]. The problem is radially symmetric with different material properties in concentric discs around the origin. The inner disc has material parameters E_1, ν_1, and the outer E_2, ν_2. At any point, the displacement vector can be written $\boldsymbol{u} = (u_r, u_\theta)$, where u_r is the radial component of the displacement and u_θ is the circumferential component. The material is subjected to a boundary displacement $\boldsymbol{u} = \boldsymbol{x}$ (in Cartesian coordinates), and the exact solution to the problem is given by (cf. [8]):

$$
u_r(r) = \begin{cases} \left(\left(1 - \dfrac{b^2}{a^2}\right)c + \dfrac{b^2}{a^2}\right) r, & 0 \le r \le a, \\ \left(r - \dfrac{b^2}{r}\right)c + \dfrac{b^2}{r}, & a \le r \le b, \end{cases}
$$

$$
u_\theta = 0,
$$

with

$$
c = \frac{(\lambda_1 + \mu_1 + \mu_2)\, b^2}{(\lambda_2 + \mu_2)\, a^2 + (\lambda_1 + \mu_1)(b^2 - a^2) + \mu_2 b^2}.
$$

We followed [8] and chose $E_1 = 1$, $\nu_1 = 0.25$, and $E_2 = 10$, $\nu_2 = 0.3$. The problem was solved on a quarter of a disc with symmetry boundary conditions on the vertical and horizontal boundaries and with the given boundary condition on the circumference.

In Fig. 1 we give the elevation of the length of the approximate displacement vector, and in Fig. 2 we show the (expected) second order L_2–convergence achieved with our method.

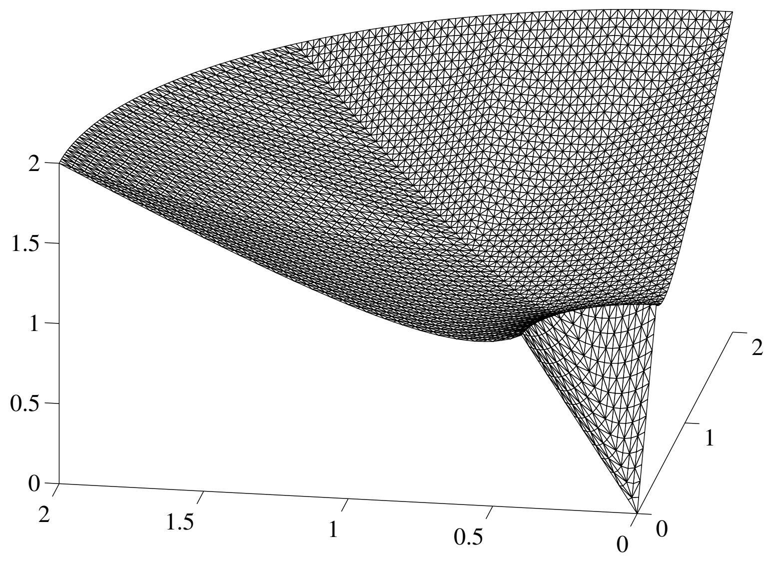

FIGURE 1. Elevation of the magnitude of the computed displacement vector on the final mesh.

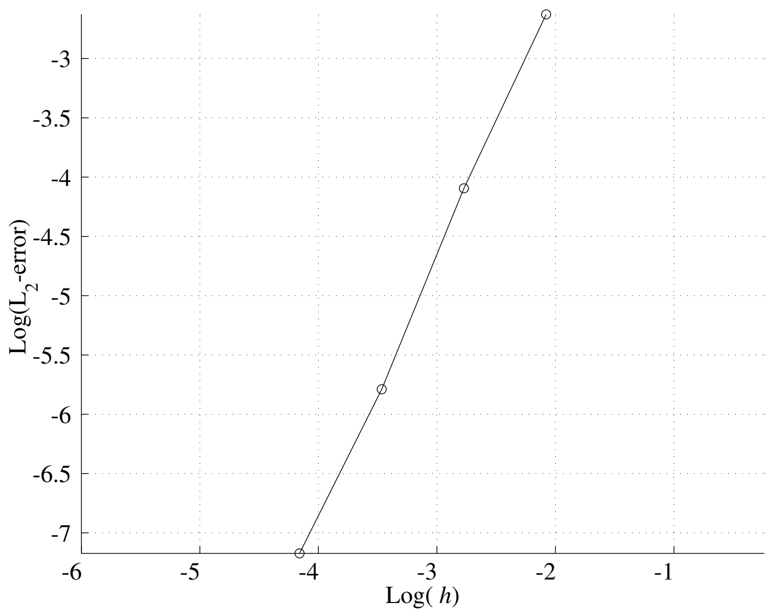

FIGURE 2. Second order convergence in $L_2(\Omega)$.

3.2. **Contact.** We considered the following model problem: find $\boldsymbol{u}$ and $\boldsymbol{\sigma}$ such that

$$\begin{aligned} \boldsymbol{\sigma} = \lambda\, \nabla\cdot\boldsymbol{u}\boldsymbol{I} + 2\mu\boldsymbol{\varepsilon}(\boldsymbol{u}) &\quad \text{in} \quad \Omega_1\cup\Omega_2,\\ -\nabla\cdot\boldsymbol{\sigma} = \boldsymbol{f} &\quad \text{in} \quad \Omega_1\cup\Omega_2,\\ \boldsymbol{u} = 0 &\quad \text{on} \quad \partial\Omega,\\ [\boldsymbol{u}\cdot\boldsymbol{n}]\le 0,\ \sigma_n\le 0,\ \sigma_n\,[\boldsymbol{u}\cdot\boldsymbol{n}] = 0,\ \boldsymbol{\sigma}_t = 0 &\quad \text{on} \quad \Gamma, \end{aligned} \tag{3.1}$$

where $\sigma_n = \boldsymbol{n}\cdot\boldsymbol{\sigma}\cdot\boldsymbol{n}$ and $\boldsymbol{\sigma}_t = \boldsymbol{\sigma}\cdot\boldsymbol{n} - \sigma_n\boldsymbol{n}$. This corresponds to the case where the inclusion is in frictionless contact with the exterior domain, and Γ plays the role of a Signorini boundary. The corresponding discrete problem is to seek $\boldsymbol{U}\in V^h$ such that

$$a_{\mathrm{c}}(\boldsymbol{U},\boldsymbol{\phi}) = L(\boldsymbol{\phi}),\quad \forall\boldsymbol{\phi}\in V^h, \tag{3.2}$$

where

$$\begin{aligned} a_{\mathrm{c}}(\boldsymbol{U},\boldsymbol{\phi}) \;:=\; & (\,\boldsymbol{\sigma}(\boldsymbol{U})\,,\boldsymbol{\varepsilon}(\boldsymbol{\phi})\,)_{\Omega_1\cup\Omega_2} - (\,[\boldsymbol{U}\cdot\boldsymbol{n}]\,,\{\boldsymbol{n}\cdot\boldsymbol{\sigma}(\boldsymbol{\phi})\cdot\boldsymbol{n}\}\,)_{\Gamma_{\mathrm{c}}} \\ & -(\,\{\boldsymbol{n}\cdot\boldsymbol{\sigma}(\boldsymbol{U})\cdot\boldsymbol{n}\}\,,[\boldsymbol{\phi}\cdot\boldsymbol{n}]\,)_{\Gamma_{\mathrm{c}}} + (\,\vartheta h^{-1}([\boldsymbol{U}\cdot\boldsymbol{n}])\,,[\boldsymbol{\phi}\cdot\boldsymbol{n}]\,)_{\Gamma_{\mathrm{c}}} \end{aligned}$$

and $\Gamma_{\mathrm{c}} = \{\boldsymbol{x}\in\Gamma:\ [\boldsymbol{U}(\boldsymbol{x})\cdot\boldsymbol{n}] > 0\}$. Here a_c is non-linear and resembles the linear form $a_{\boldsymbol{S}_h}$ with $\boldsymbol{K}=0$. We can identify $\vartheta := \delta$ in Lemma 4, and thus the discrete problem can be made coercive as long as the physical problem is well–posed.

In order to realize a solution procedure for this problem, we checked after each iteration whether the discrete solution violates $[\boldsymbol{U}\cdot\boldsymbol{n}]\le 0$ or not. Wherever this condition was violated we assumed that we were at Γ_c, and elsewhere we assumed a traction-free boundary. An alternative would be to also check the sign of σ_n; this was not done in our implementation. We used a fixed point iteration scheme which does not necessarily converge since points in contact at one iteration may not be in contact in the next (a common problem in contact computations). Thus we stopped the iterations when the difference between two consecutive solutions are three orders of magnitude smaller than the solution after the first iteration.

For our numerical example shown in Fig. 3, we considered a domain $(0,1/2)\times(0,1)$, with $u_x = 0$ at $x=0$, $\boldsymbol{u}=\boldsymbol{0}$ at $y=0$, and $\boldsymbol{u}=(0,-0.1)$ at $y=1$. In this domain, we considered a circular inclusion with higher stiffness than the surrounding material. The elasticity parameters were chosen as $\nu = 0.3$, $E_{\min} = 10^6$, $E_{\max} = 10^7$. $\vartheta = 10\,E_{\max}$.

3.3. **Crack propagation.** Finally, we considered a simple rigid-hardening model for crack formation. We defined $\sigma_{\max}$ as the maximum positive eigenvalue of the matrix $\sigma_{ij}(\boldsymbol{u})$ of the components of $\boldsymbol{\sigma}(\boldsymbol{u})$ and assumed that as long as $\sigma_{\max} < \sigma_{\mathrm{c}}$, where σ_{c} was a threshold value, we had $[\boldsymbol{u}] = 0$ at the crack tip. When $\sigma_{\max}\ge\sigma_{\mathrm{c}}$, the crack (defining Γ) was assumed to run perpendicularly to the eigenvector associated with $\sigma_{\max}$ and the constitutive relation changed to $[\boldsymbol{u}] = -\boldsymbol{K}\{\boldsymbol{\sigma}(\boldsymbol{u})\cdot\boldsymbol{n}\}$. The physical problem modeled by these constitutive relations is a solid that can withstand high compression but cracks in high tension and which retains a certain stiffness in the crack zone even after crack opening. We chose this model for its simplicity; obviously, the computational framework allows for more physically realistic models. We remark that Γ changed during the computation, so again we had a nonlinear problem.

As regards the implementation, we let the crack entering an element cause a discontinuity in the whole of the element. The crack was assumed to follow a straight line through each element until it hit the boundary to the next element. The situation is illustrated in Fig. 4, where the line C–D is the crack, obeying the constitutive relation $[\boldsymbol{u}] = -\boldsymbol{K}\{\boldsymbol{\sigma}(\boldsymbol{u})\cdot\boldsymbol{n}\}$. The line A–B, along which the solution should be continuous, was handled as an ordinary interface, i.e., with $\boldsymbol{K}=0$. Note that continuity was enforced at the nodes A and B,

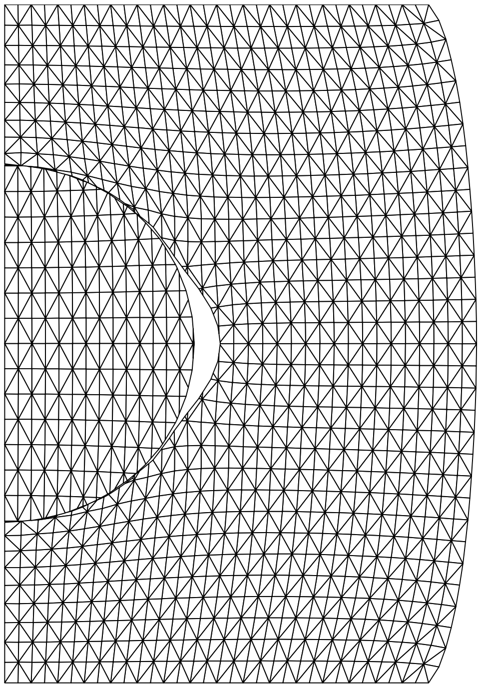

FIGURE 3. Displacements for the contact problem

which localized the effect of the discontinuity since then all non-cracked elements could be standard continuous elements.

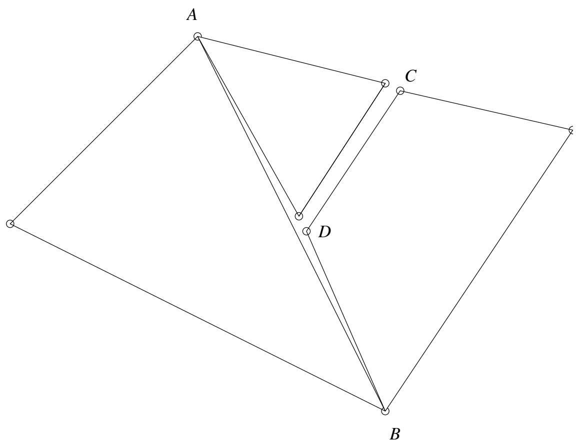

FIGURE 4. Illustration of the handling of a cracked element.

For our numerical example, we chose a domain $(-1, 2) \times (-1, 2)$, fixed at $y = -1$ and traction free elsewhere. A body force $\boldsymbol{f} = (-10^6, 0)$ was acting on the console, and the data for this problem were chosen as $\nu = 0.3$, $E = 10^9$ After crack formation, we assumed a residual compliance corresponding to $\alpha = \beta = 5 \times 10^{-9}$. The small compliancy on the crack interface was necessary in order to regularize the problem; the constant strain elements used proved to be very sensitive to the crack tip singularity and we experienced problems in getting any useful information out of the stresses for large values of α and β. This typically resulted in the crack turning back on itself. Clearly, there is a need for special approximations in the vicinity of the crack tip. Such approximations can very conveniently be invoked using the discontinuous Galerkin concept already inherent in the method, although this is beyond the scope of this paper. An alternative possibility in the case of brittle cracks could be to use energy methods, such as the J-integral, which do not require a good resolution at the crack tip.

In Figure 5 we show the successive growth of a crack forcefully initiated at $x = 2$, $y = 0.72$.

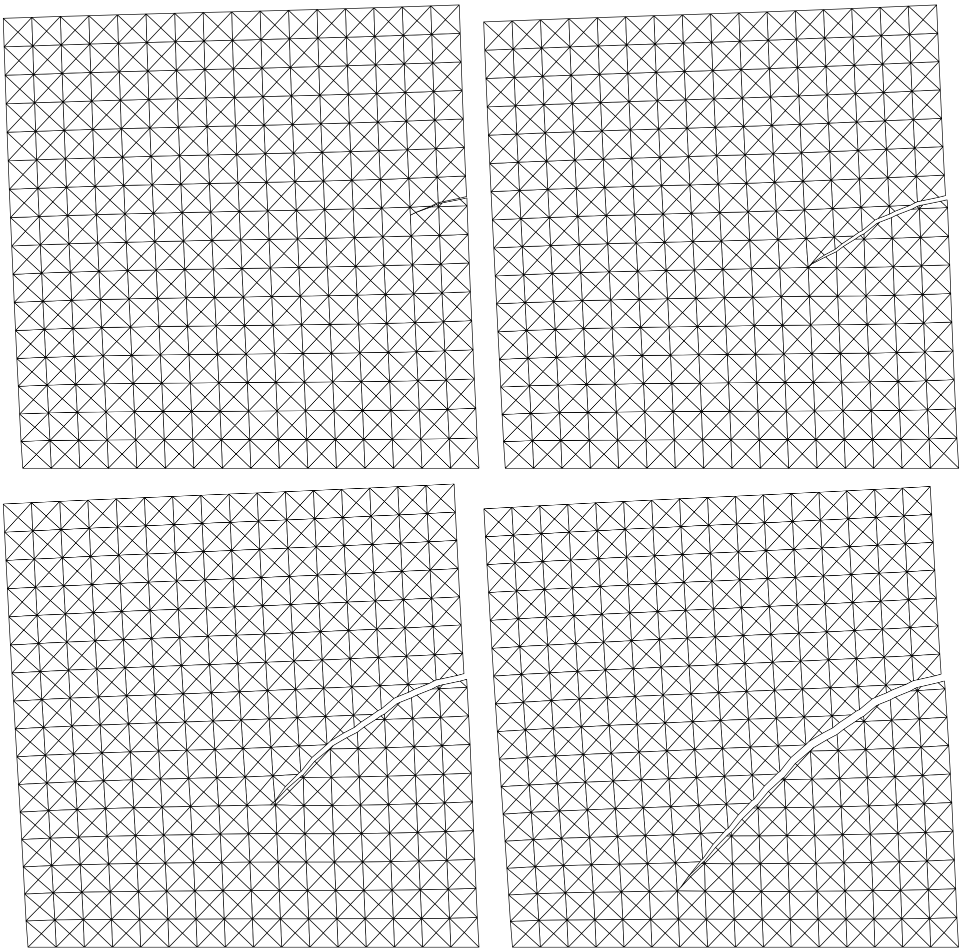

FIGURE 5. Crack propagation.

4. Concluding remarks

We have suggested a new discontinuous finite element approach for the simulation of weak and strong discontinuities in linear and nonlinear elasticity. The method has been shown to have optimal convergence in the linear case, under the usual regularity requirements. Unlike the current mainstream approaches, our method requires only piecewise polynomial *ansatz* functions, though special purpose approximations can easily be incorporated.

For nonlinear problems, such as contact and crack propagation, we have given formulations and examples in model situations. These serve to show the potential of the methodology; future work will focus on more realistic models.

References

[1] I. Babuška, *The finite element method for elliptic equations with discontinuous coefficients*, Computing, 5 (1970), pp. 207–213.

[2] T. Belytschko T, N. Möes, S. Usui , and C. Parimi, *Arbitrary discontinuities in finite elements.* Internat. J. Numer. Methods Engrg., 50 (2001), pp. 993–1013.

[3] A. Hansbo and P. Hansbo, *An unfitted finite element method, based on Nitsche's method, for elliptic interface problems*, Comput. Methods Appl. Mech. Engrg., 191 (2002) 5537–5552.

[4] B.L. Karihaloo and Q.Z. Xiao, *Modelling of stationary and growing cracks in FE framework without remeshing: a state-of-the-art review*, Comput. Struct., 81 (2003) 119–129.

[5] D. Leguillon and E. Sanchez-Palencia, *Computation of Singular Solutions in Elliptic Problems and Elasticity.* Wiley, 1987.

[6] J. Nitsche, *Über ein Variationsprinzip zur Lösung von Dirichlet-Problemen bei Verwendung von Teilräumen, die keinen Randbedingungen unterworfen sind*, Abh. Math. Sem. Univ. Hamburg, 36 (1971), pp. 9–15.

[7] R. Stenberg, Presentation at the Oberwolfach meeting on Discontinuous Galerkin Methods, 2002 (Unpublished).

[8] N. Sukumar, D.L. Chopp, N. Möes, and T. Belytschko, *Modeling holes and inclusions by level sets in the extended finite-element method*, Comput. Methods Appl. Mech. Engrg., 190 (2001) 6183–6200.

[9] V. Thomée, *Galerkin Finite Element Methods for Parabolic Problems.* Springer-Verlag, 1997.

[10] G. N. Wells and L. J. Sluys, *A new method for modelling cohesive cracks using finite elements*, Internat. J. Numer. Methods Engrg., 50 (2001), pp. 2667–2682.

[11] Z. Zhong and S. A. Meguid, *On the imperfectly bonded spherical inclusion problem*, J. Appl. Mech., 66 (1999), pp. 839–846.

Chalmers Finite Element Center Preprints

2001–01 *A simple nonconforming bilinear element for the elasticity problem*
Peter Hansbo and Mats G. Larson

2001–02 *The $\mathcal{LL}^*$ finite element method and multigrid for the magnetostatic problem*
Rickard Bergström, Mats G. Larson, and Klas Samuelsson

2001–03 *The Fokker-Planck operator as an asymptotic limit in anisotropic media*
Mohammad Asadzadeh

2001–04 *A posteriori error estimation of functionals in elliptic problems: experiments*
Mats G. Larson and A. Jonas Niklasson

2001–05 *A note on energy conservation for Hamiltonian systems using continuous time finite elements*
Peter Hansbo

2001–06 *Stationary level set method for modelling sharp interfaces in groundwater flow*
Nahidh Sharif and Nils-Erik Wiberg

2001–07 *Integration methods for the calculation of the magnetostatic field due to coils*
Marzia Fontana

2001–08 *Adaptive finite element computation of 3D magnetostatic problems in potential formulation*
Marzia Fontana

2001–09 *Multi-adaptive galerkin methods for ODEs I: theory & algorithms*
Anders Logg

2001–10 *Multi-adaptive galerkin methods for ODEs II: applications*
Anders Logg

2001–11 *Energy norm a posteriori error estimation for discontinuous Galerkin methods*
Roland Becker, Peter Hansbo, and Mats G. Larson

2001–12 *Analysis of a family of discontinuous Galerkin methods for elliptic problems: the one dimensional case*
Mats G. Larson and A. Jonas Niklasson

2001–13 *Analysis of a nonsymmetric discontinuous Galerkin method for elliptic problems: stability and energy error estimates*
Mats G. Larson and A. Jonas Niklasson

2001–14 *A hybrid method for the wave equation*
Larisa Beilina, Klas Samuelsson and Krister Åhlander

2001–15 *A finite element method for domain decomposition with non-matching grids*
Roland Becker, Peter Hansbo and Rolf Stenberg

2001–16 *Application of stable FEM-FDTD hybrid to scattering problems*
Thomas Rylander and Anders Bondeson

2001–17 *Eddy current computations using adaptive grids and edge elements*
Y. Q. Liu, A. Bondeson, R. Bergström, C. Johnson, M. G. Larson, and K. Samuelsson

2001–18 *Adaptive finite element methods for incompressible fluid flow*
Johan Hoffman and Claes Johnson

2001–19 *Dynamic subgrid modeling for time dependent convection–diffusion–reaction equations with fractal solutions*
Johan Hoffman

2001–20 *Topics in adaptive computational methods for differential equations*
Claes Johnson, Johan Hoffman and Anders Logg

2001–21 *An unfitted finite element method for elliptic interface problems*
Anita Hansbo and Peter Hansbo

2001–22 *A P^2–continuous, P^1–discontinuous finite element method for the Mindlin-Reissner plate model*
Peter Hansbo and Mats G. Larson

2002–01 *Approximation of time derivatives for parabolic equations in Banach space: constant time steps*
Yubin Yan

2002–02 *Approximation of time derivatives for parabolic equations in Banach space: variable time steps*
Yubin Yan

2002–03 *Stability of explicit-implicit hybrid time-stepping schemes for Maxwell's equations*
Thomas Rylander and Anders Bondeson

2002–04 *A computational study of transition to turbulence in shear flow*
Johan Hoffman and Claes Johnson

2002–05 *Adaptive hybrid FEM/FDM methods for inverse scattering problems*
Larisa Beilina

2002–06 *DOLFIN - Dynamic Object oriented Library for FINite element computation*
Johan Hoffman and Anders Logg

2002–07 *Explicit time-stepping for stiff ODEs*
Kenneth Eriksson, Claes Johnson and Anders Logg

2002–08 *Adaptive finite element methods for turbulent flow*
Johan Hoffman

2002–09 *Adaptive multiscale computational modeling of complex incompressible fluid flow*
Johan Hoffman and Claes Johnson

2002–10 *Least-squares finite element methods with applications in electromagnetics*
Rickard Bergström

2002–11 *Discontinuous/continuous least-squares finite element methods for elliptic problems*
Rickard Bergström and Mats G. Larson

2002–12 *Discontinuous least-squares finite element methods for the Div-Curl problem*
Rickard Bergström and Mats G. Larson

2002–13 *Object oriented implementation of a general finite element code*
Rickard Bergström

2002-14 *On adaptive strategies and error control in fracture mechanics*
Per Heintz and Klas Samuelsson

2002-15 *A unified stabilized method for Stokes' and Darcy's equations*
Erik Burman and Peter Hansbo

2002-16 *A finite element method on composite grids based on Nitsche's method*
Anita Hansbo, Peter Hansbo and Mats G. Larson

2002-17 *Edge stabilization for Galerkin approximations of convection–diffusion problems*
Erik Burman and Peter Hansbo

2002-18 *Adaptive strategies and error control for computing material forces in fracture mechanics*
Per Heintz, Fredrik Larsson, Peter Hansbo and Kenneth Runesson

2002-19 *A variable diffusion method for mesh smoothing*
J. Hermansson and P. Hansbo

2003-01 *A hybrid method for elastic waves*
L.Beilina

2003-02 *Application of the local nonobtuse tetrahedral refinement techniques near Fichera-like corners*
L.Beilina, S.Korotov and M. Křížek

2003-03 *Nitsche's method for coupling non-matching meshes in fluid-structure vibration problems*
Peter Hansbo and Joakim Hermansson

2003-04 *Crouzeix–Raviart and Raviart–Thomas elements for acoustic fluid–structure interaction*
Joakim Hermansson

2003-05 *Smoothing properties and approximation of time derivatives in multistep backward difference methods for linear parabolic equations*
Yubin Yan

2003-06 *Postprocessing the finite element method for semilinear parabolic problems*
Yubin Yan

2003-07 *The finite element method for a linear stochastic parabolic partial differential equation driven by additive noise*
Yubin Yan

2003-08 *A finite element method for a nonlinear stochastic parabolic equation*
Yubin Yan

2003-09 *A finite element method for the simulation of strong and weak discontinuities in elasticity*
Anita Hansbo and Peter Hansbo

These preprints can be obtained from

`www.phi.chalmers.se/preprints`